



# Recent advances in cardiac positron emission tomography for quantitative perfusion analyses and molecular imaging

Osamu Manabe<sup>1,2</sup> · Masanao Naya<sup>3</sup> · Tadao Aikawa<sup>2,4</sup> · Nagara Tamaki<sup>5</sup>

Received: 9 June 2020 / Accepted: 31 August 2020 / Published online: 11 September 2020  
© The Japanese Society of Nuclear Medicine 2020

## Abstract

Positron emission tomography (PET) has been used to noninvasively evaluate myocardial perfusion and metabolism. For clinical assessments of myocardial perfusion, the quantitative capability of PET permits precise assessments of ischemia and microcirculatory dysfunction, playing an important role in patient management and outcome analyses. <sup>18</sup>F-fluorodeoxyglucose (FDG) PET has recently been used to identify active cardiovascular lesions such as cardiac sarcoidosis, endocarditis, and aortitis. This may hold promise for the early and accurate diagnosis of such fatal diseases, as well as for patient management. This review covers new and clinical roles of cardiac PET in treatment strategies and patient outcomes.

**Keywords** Cardiac PET · Myocardial blood flow · Active myocardial lesions · Quantitative analysis

## Introduction

With the rapid development of imaging modalities, a variety of new applications for the noninvasive imaging of cardiac diseases have appeared [1, 2]. Positron emission tomography (PET) has long been used as a functional imaging modality that uses several PET tracers to target perfusion, metabolism, innervation, and inflammatory conditions [3–8]. More recently, this imaging technique has played important roles in many clinical conditions such as early clinical diagnosis, patient management, and monitoring treatment response [9]. Here we review the recent clinical applications of cardiac PET for cardiovascular diseases, with a focus on quantitative

myocardial perfusion imaging and inflammatory imaging using PET.

## Advantages of PET perfusion assessments

PET has a number of advantages. It provides higher quality myocardial perfusion images than conventional single-photon emission computed tomography (SPECT) imaging. PET myocardial perfusion imaging (MPI) thus provides more accurate diagnostic values and a higher incremental prognostic value than SPECT–MPI in patients with coronary artery disease (CAD) [10–13]. Another major advantage of PET over SPECT is the ability to quantify tracer concentrations. PET, therefore, permits the quantitative analysis of myocardial blood flow (MBF; in mL per g per min) and the myocardial flow reserve (MFR: as the ratio of the MBF at peak hyperemia to the MBF at rest), using a suitable radiotracer kinetic model. Along with perfusion imaging and coronary angiography, quantitative MBF and MFR values provide cardiologists with unique insights into diagnostic and prognostic values (Fig. 1). In fact, there has been growing evidence of the usefulness of the MBF and MFR in assessments of CAD patients [14–17].

Since MBF and MFR analyses play important roles in determining the severity of CAD, a quantitative analysis similar to that used for the MBF has been reported in the uses of dynamic acquisition with cardiac computed

✉ Masanao Naya  
naya@med.hokudai.ac.jp

<sup>1</sup> Department of Diagnostic and Interventional Radiology, Hokkaido University Hospital, Sapporo, Japan

<sup>2</sup> Department of Radiology, Saitama Medical Center, Jichi Medical University, Saitama, Japan

<sup>3</sup> Department of Cardiovascular Medicine, Faculty of Medicine and Graduate School of Medicine, Hokkaido University, Kita-15, Nishi-7, Kita-ku, Sapporo 060-8638, Japan

<sup>4</sup> Cardiovascular Research Center, Icahn School of Medicine At Mount Sinai, New York, NY, USA

<sup>5</sup> Department of Radiology, Kyoto Prefectural University of Medicine, Kyoto, Japan

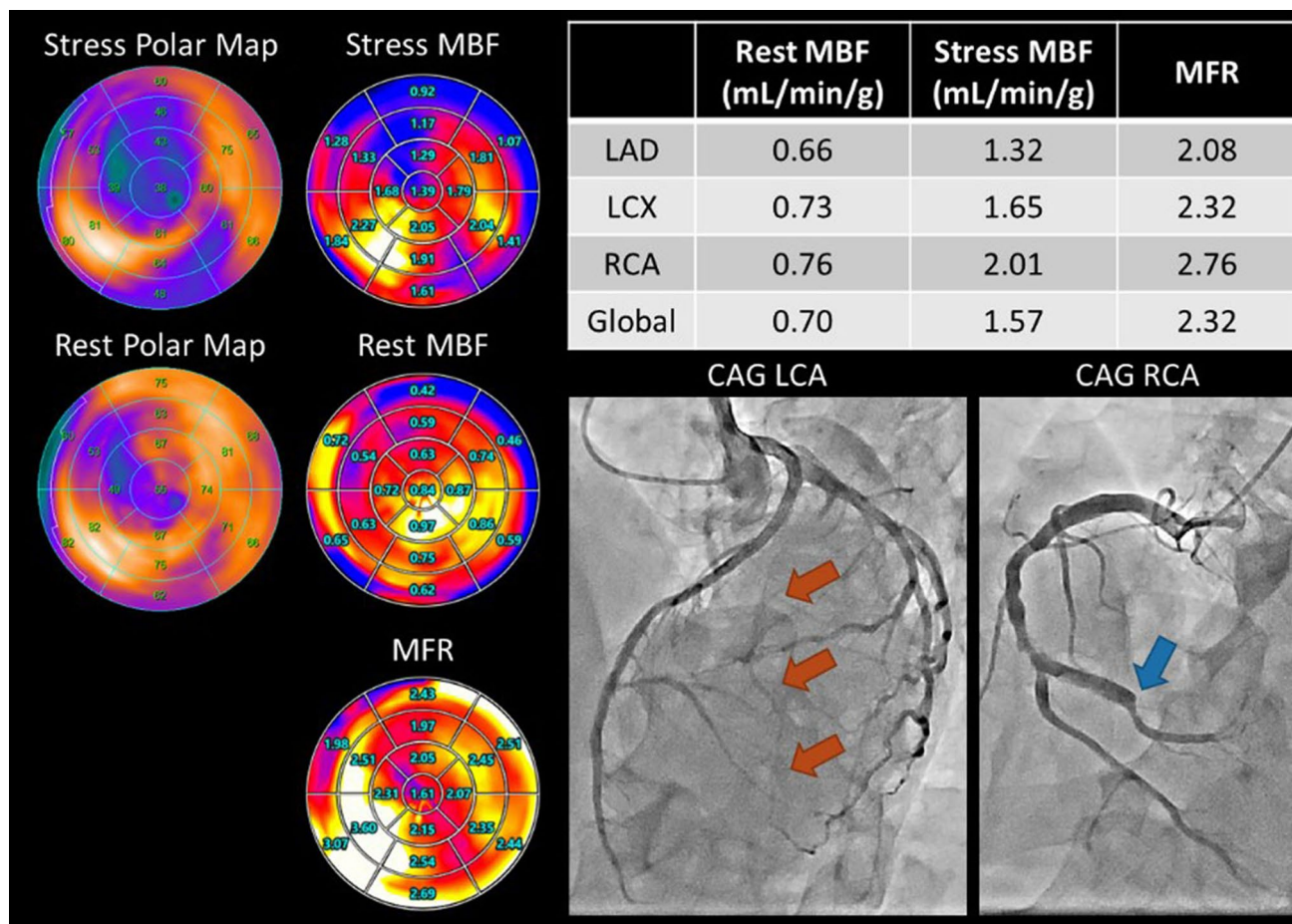


**Fig. 1** This patient had a history of myocardial infarction in the left anterior descending (LAD) artery. In the chronic phase,  $^{13}\text{N}$ -ammonia PET/CT revealed severe myocardial perfusion defects in the broad anterior and inferior walls during stress, which are partially reversible at rest (left figure). Quantitative myocardial blood flow at rest and

stress were estimated (right upper figure). Invasive coronary angiography showed that the main LAD was patent, but the diagonal branch was jeopardized by the stent of the LAD and the obstructive posterolateral branch of the right coronary artery (bottom right)

tomography (CT), magnetic resonance imaging (MRI), and SPECT with a kinetic model analysis similar to that used with PET [18–22]. Most of the quantitative parameters have been validated by a comparison with cardiac PET. Such quantitative analyses may add important value to CAD assessments in addition to the coronary structure and myocardial functional analyses afforded by CT and MRI. On the other hand, CT and MRI contrast agents, as well as SPECT perfusion tracers, may not be suitable for the quantitative assessments of the MBF since the extraction fractions of contrast agents are not very high in the high-flow range compared to commonly used PET tracers such as O-15 water and N-13 ammonia [10, 18, 19, 23]. Doppler echocardiography can be used to estimate the coronary flow (velocity) reserve based on the vasodilator capacity, defined as the ratio of the maximal hyperemic coronary blood flow to the resting flow [24, 25].

### PET applications for risk analyses and interventional therapy

The MFR estimated by PET has emerged as a powerful marker of the risk for adverse cardiovascular outcomes including cardiac death [14, 15, 26, 27]. The MFR is an integrated measure of the entire coronary vasculature, reflecting epicardial coronary anatomy and microvascular dysfunction [28]. Using the fractional flow reserve (FFR) is another approach to evaluations of the functional consequences of coronary stenosis; a determination of the FFR measures the pressure differences across a coronary artery stenosis during maximum hyperemia [29]. Since coronary angiography is often insufficient in guiding a percutaneous coronary intervention (PCI) procedure, the FFR has gained wide acceptance for estimating whether a coronary lesion may cause myocardial ischemia requiring coronary revascularization.

The DEFER study, which included subjects with stable chest pain, showed that a prognostic factor of CAD was the ability to induce myocardial ischemia as reflected by an FFR < 0.75, whereas a prognosis of FFR  $\geq$  0.75 was excellent and the risk of cardiac death or myocardial infarction related to the stenosis was < 1% per year and was not decreased by stenting [30]. The FAME (Fractional Flow Reserve Versus Angiography for Multivessel Evaluation) study involving 1005 patients with multivessel CAD demonstrated that functional consequences of coronary stenoses revealed by the FFR were associated with significantly lower morbidity and mortality than a PCI guided only by anatomical coronary stenosis [31, 32]. Both the DEFER and FAME studies re-emphasized the importance of assessing the physiologic stenosis of the coronary artery.

A number of studies show a correlation between the MFR and FFR for estimating the functional significance of coronary stenosis. An initial comparison study revealed a close correlation between the MFR and FFR in patients with mostly single-vessel stenosis [33]. A quantitative estimation of the severity of stenosis by MFR does not depend on an intervessel comparison even for multivessel disease. However, several studies of patients with multivessel disease showed modest (not high) agreement between their MFR and FFR values [34].

Discordance between the MFR and FFR is explained in part by the fact that the FFR is a specific index of the epicardial artery, whereas the MFR is influenced not only by epicardial stenosis but also by microvascular disease [35]. In that study, the relative expansion of focal and diffuse disease reflected the linearity of the relationship between the MFR and FFR. Lesions with both an FFR  $\geq$  0.8 and an MFR  $\geq$  2.0 were concordant for the normal coronary artery, and lesions with both an FFR < 0.75 and an MFR < 2.0 were concordant for CAD with focal stenosis and microvascular disorder. Lesions with discordant MFR and FFR values (i.e., FFR < 0.75 and MFR  $\geq$  2.0, FFR  $\geq$  0.8 and MFR < 2.0) may reflect the degree and extent of focal and diffuse disease [36].

It is quite important to determine whether the MFR can be used to select appropriate CAD patients for optimal medical therapy (OMT), percutaneous coronary intervention (PCI), or coronary artery bypass grafting (CABG). Since the MFR is an integrated measure of the entire coronary vasculature, reflecting the epicardial coronary anatomy and microvascular dysfunction, both coronary revascularization and medical therapy may increase the MFR. Importantly, several studies have demonstrated that coronary revascularization for CAD is associated with early post-procedural improvements in the regional MFR [37–40]. Conversely, in a single-center retrospective study, a prognostic difference between CABG and PCI was seen only among patients with very low MFRs [15]. That study observed good outcomes

for the patients with a preserved MFR by OMT, PCI, or CABG but significantly different outcomes for those with a reduced MFR, indicating microvascular dysfunction. The study's authors suggested that CABG may be a suitable treatment for these patients, with better outcomes than PCI or OMT [15]. The study assessed a total of 329 consecutive patients including patients with diabetes mellitus (40.1%), hypertension (88.2%), and dyslipidemia (73.3%), which indicates that much of the patients had an increased risk of microvascular dysfunction. For patients with microvascular dysfunction and CAD comorbid conditions, complete revascularization with CABG might be a more effective approach for global cardiovascular risk reduction. Although it was a single-center observational study, its results offer important insights into how to manage CAD patients, particularly those with microvascular dysfunction. In addition, a quantitative MFR analysis by PET should play an important role in appropriately managing many CAD patients [41].

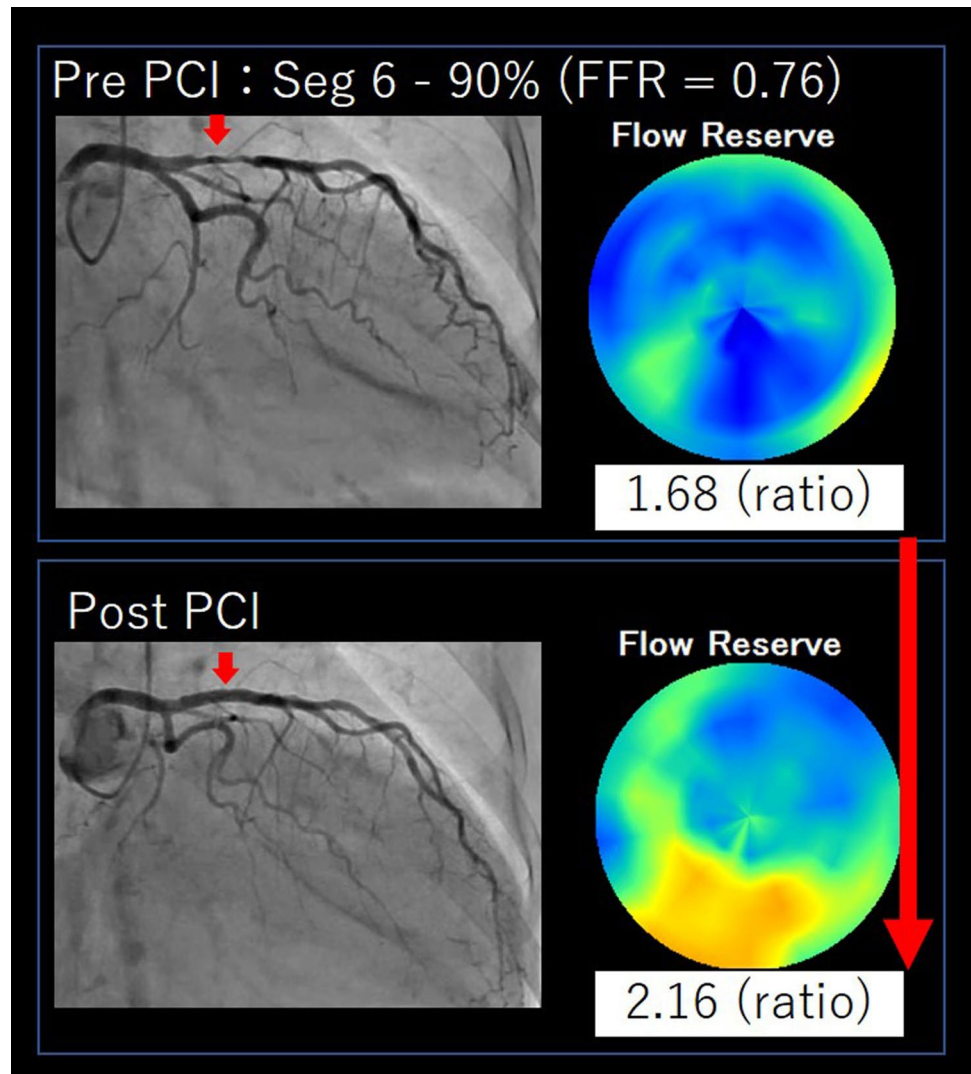
We have analyzed global and regional MFR values before and 6 months after coronary revascularization using O-15 water PET in patients with obstructive CAD [17, 42] (Fig. 2). We observed a significant increase in the MFR only in the patients undergoing CABG (not OMT or PCI) in general. Among the patients with a reduced MFR (< 2.0), both PCI and CABG significantly improved the MFR [17]. The increases in global and regional MFR values were correlated with the degree of angiographic improvement after coronary revascularization. Such improvement was not related to the presence of subendocardial infarction assessed by MRI [42]. Given the fact that the effects of coronary revascularization depended on both the angiographic CAD burden before revascularization and the degree of angiographic improvement after revascularization, complete revascularization has great potential to improve the MFR in patients with high-risk CAD.

## Molecular imaging using PET

PET has a great advantage over any other noninvasive imaging for performing various types of molecular imaging.  $^{18}\text{F}$ -fluorodeoxyglucose (FDG)-PET has long been used for cardiovascular diseases. One of the classical applications of PET is for myocardial viability assessments. FDG-PET assesses glucose metabolism in the heart and thus the myocardial viability [43–46]. A region with preserved FDG uptake indicates the presence of viable myocardium. For this purpose, glucose administration with oral loading or an insulin–glucose clamp is applied to increase the FDG uptake in both the normal and ischemic but viable myocardium, whereas it does not induce FDG uptake in infarcted tissue.

FDG-PET has also been used to identify active inflammatory lesions, because glucose is also consumed in the inflammatory process [47, 48]. Depending on the

**Fig. 2** The left figure shows a patient with obstructive disease in the left anterior descending artery. Six months after a percutaneous coronary intervention (PCI) with optical medical therapy, the global MFR increased



purposes of in vivo functional imaging, patients should be prepared carefully before the administration of FDG [49, 50]. Postprandial condition, glucose loading, or an insulin clamp is applied for a myocardial viability assessment in which FDG accumulates in both normal and ischemic but viable myocardium. A long fasting period with or without the administration of heparin is required to identify active inflammatory lesions with suppressed physiological myocardial FDG uptake. Patient preparation before the FDG administration is quite important since the FDG uptake in the myocardium is dependent on either the physiological uptake or an abnormal active uptake depending on the patient's condition. The activation of granulocytes and macrophages during inflammation enhances the uptake of FDG. Thus, FDG-PET is useful for detecting active cardiovascular inflammation [47, 51].

### PET applications for assessing active cardiovascular lesions

Sarcoidosis is a noncaseating granulomatous disease with multi-organ involvement and generally a good prognosis. However, cardiac involvement in sarcoidosis is often associated with morbidity and death, mainly as a result of left ventricular dysfunction and arrhythmia such as ventricular tachyarrhythmia and conduction disturbance [52, 53]. Because of the lower sensitivity of histopathology-based diagnoses, imaging tools are important for the evaluation of cardiac sarcoidosis. In Japan, guidelines for the diagnosis of cardiac sarcoidosis were first published in 1992, and even in the 2006 revision of the guidelines, FDG-PET was not included in the diagnostic criteria. With the technological progress and the establishment of its usefulness for cardiac

sarcoidosis, FDG-PET was approved in 2012 by the Japanese Ministry of Health, Labour and Welfare and covered by insurance as an assessment tool for inflammatory cardiac sites. The guidelines for the diagnosis and treatment of cardiac sarcoidosis published in 2019 by the Japanese Society of Nuclear Cardiology included FDG-PET findings for one of the major criteria [54].

FDG-PET has been considered a useful tool for identifying cardiac and other organ involvement. The accumulation of FDG is associated with an active inflammatory process, thus allowing for the activity of the inflammatory disease to be evaluated [55–58] (Fig. 3). The Heart Rhythm Society (HRS) and the Japanese Society of Nuclear Cardiology (JSNC) recommend using FDG-PET and cardiovascular magnetic resonance (CMR) for the diagnosis of cardiac sarcoidosis [59, 60]. The late gadolinium enhancement (LGE) technique using CMR relies on the delivery of a chelated gadolinium contrast agent to the myocardium. This agent is biologically inert and distributes freely in the extracellular space. Therefore, a relative accumulation of the agent is seen in areas with increased extracellular volume such as fibrotic scars and sites of the formation of a non-caseating

epithelioid cell granuloma in the delayed images [61]. Since the accumulation mechanisms of FDG and MRI contrast media are different, the information obtained does not necessarily correspond [62, 63].

The assessment of LGE is also valuable in the prognosis of cardiac sarcoidosis [64]. The combination of FDG and perfusion evaluation is useful not only for improving the accuracy of diagnoses but also for the predicting the outcomes of cardiac sarcoidosis [65]. A digital PET/CT scanner with high spatial resolution can improve the detection of patchy sarcoidosis lesions in the heart. In this case, digital PET clearly delineates epicardial and endocardial lesions at the left ventricle as well as patchy lesions at the right ventricular free wall in accord with the magnitude of severity, similar to the case with MRI (Fig. 3). Right ventricular FDG uptake may be more specific in the diagnosis of cardiac sarcoidosis [66], suggesting that digital PET/CT has the potential to improve the diagnosis of cardiac sarcoidosis (Fig. 3).

It is important to have patients fast for a long period to minimize the physiological FDG uptake in the myocardium for the assessment of cardiac sarcoidosis [50]. The long fasting and dietary modification prior to FDG-PET are important to suppress the physiological myocardial uptake, which provides major potential for a false-positive diagnosis of cardiac sarcoidosis. The JSNC states that the preparation of the patient for an FDG-PET examination should include a low-carbohydrate diet (< 5 g of carbohydrates) and prolonged fasting (a minimum of 12 h but up to 18 h if possible). A high-fat diet 3–6 h before the administration of FDG remains to be established, but there might be another approach to suppress the physiological myocardial uptake [54].

There have been a number of attempts to evaluate active cardiac sarcoidosis with no physiological myocardial uptake with the use of other PET tracers, including  $^{18}\text{F}$ -fluorothymidine (FLT) and  $^{18}\text{F}$ -fluoromisonidazole (FMISO) [67–70]. Although their uptake in active myocardial lesions is lower with these new techniques compared to the use of FDG, these other tracers have the potential to diagnose specific active sarcoidosis. In addition, these techniques may hold promise for identifying other active myocardial lesions—such as myocarditis—similar to FDG-PET.

Infective endocarditis can cause another type of severe cardiac inflammation, in which the diagnosis and management by FDG-PET plays important roles. Echocardiography, the mainstay for the diagnosis of infective endocarditis, can detect only structural damage in the heart. In addition to local damage in the myocardium, a metastatic infection, embolic phenomenon, or immune-mediated damage may result in considerable morbidity and mortality. In many cases, endocarditis can often be associated with a prosthetic valve. Cardiac CT and MRI thus have an inherent limitation for accurate image analyses. FDG-PET, in contrast, is a powerful tool not only for identifying active myocardial

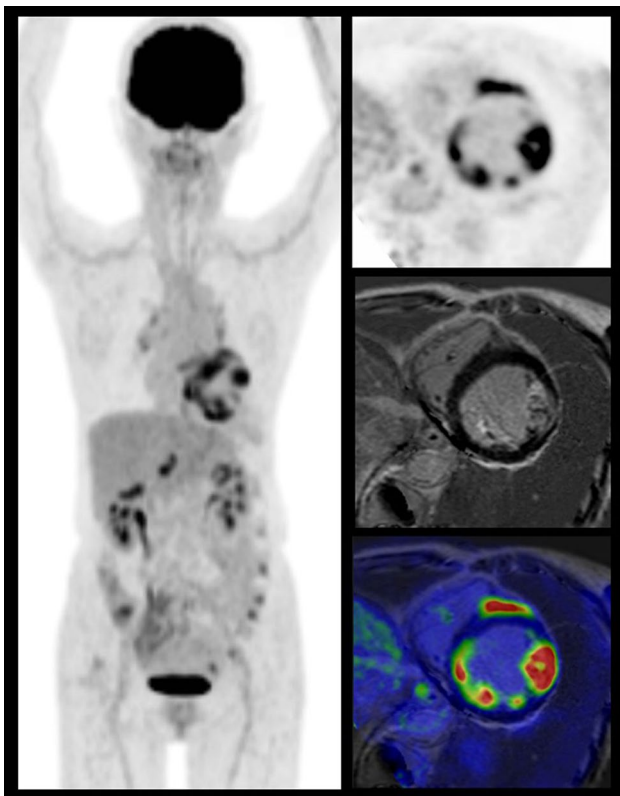


**Fig. 3** A case of cardiac sarcoidosis scanned by a digital PET/CT scanner. Significant FDG uptake concordant with late gadolinium enhancement was observed by MRI. Digital PET improves the spatial resolution and might be useful to detect small inflammatory sarcoidosis lesions

lesions but also for detecting metastatic and embolic lesions throughout the body based on a whole-body PET survey [71–76]. In a meta-analysis of 13 studies involving 537 patients, PET/CT showed moderate sensitivity and specificity for the diagnosis of infective endocarditis [76]. However, the sensitivity improved when patients with suspected prosthetic-valve endocarditis were evaluated. These findings suggest that PET/CT has the potential to serve as an adjunctive diagnostic modality in challenging cases of possible infective endocarditis.

Aortitis is a generic term; it is defined as an inflammatory condition of infectious or noninfectious origin involving the aortic wall, such as Takayasu's arteritis, giant cell arteritis, and IgG4 autoimmune arteritis. This inflammatory process may deteriorate the aortic wall, resulting in potentially life-threatening vascular complications. It is, therefore, important to establish a diagnosis as early as possible. FDG-PET imaging has been used to accurately detect vascular inflammation in the aortic wall (Fig. 4), [77–83], and FDG-PET is considered a valuable tool for monitoring treatment effects in this disease.

FDG-PET/CT is widely used for the diagnosis, staging, and treatment response assessment for a wide range of hematologic and solid cancers (Figs. 5, 6). FDG-PET can be used for the noninvasive differentiation of benign and malignant cardiac tumors because most types of malignant tumors show increased glucose metabolism [84, 85]. Since CT and MRI also play important roles for this purpose, a combined analysis of anatomical/functional and molecular imaging should be applied to obtain an accurate diagnosis, to identify the tumor's location, for treatment planning, and for the treatment monitoring of cardiac tumors using integrated PET/CT and/or PET/MRI imaging [86, 87].

FDG-PET is commonly performed about 1 h after the administration of FDG in general clinical practice, mainly in oncological areas. However, an FDG-PET examination for cardiovascular imaging, PET imaging is preferably performed 90–120 min after the FDG administration. Residual blood pool activity remains with a slow blood pool clearance of FDG after a long fasting period. Better lesion contrast may thus be obtained slightly later than the conventional time after FDG administration [88].

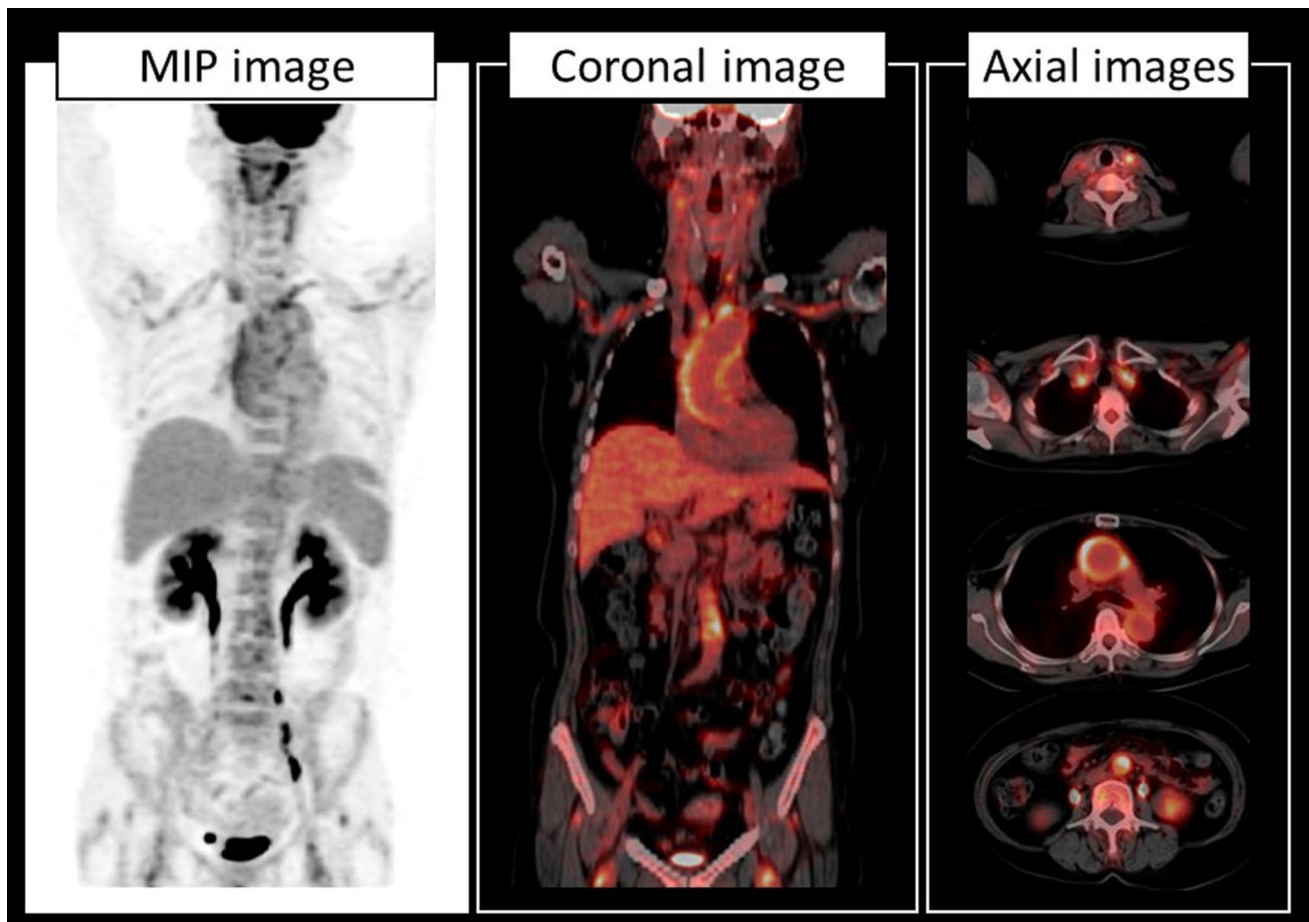


**Fig. 4** A female in her 60 s presented with a 1-month history of unknown fever. The FDG PET/CT images showed intense uptake in the wall of the aorta, bilateral subclavian arteries, and common carotid artery compatible with a diagnosis of giant cell arteritis

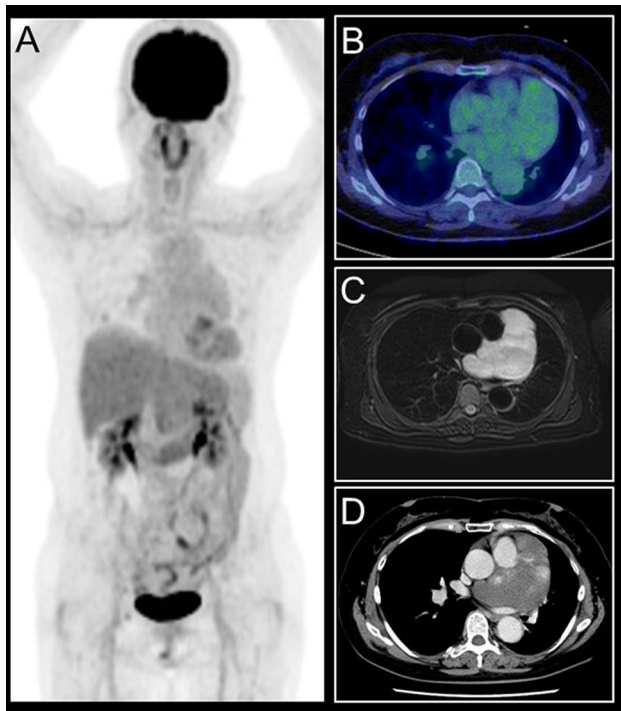


**Fig. 5** A case of pericardial capillary haemangioma. The bulky mass attached to the anterior wall of the left ventricle showed low FDG uptake similar to a blood pool (**a**, **b**), a homogeneous hyperintense signal in T2-weighted image (**c**), and nodular enhancement on contrast-enhanced CT (**d**)

## Summary

Cardiac PET is a powerful noninvasive imaging technique that is increasingly used across clinical settings. For the clinical assessment of myocardial perfusion, the quantitative capability of PET permits the precise assessment of ischemia and microcirculatory dysfunction, which indicates an important role for PET in patient management and outcome analyses. In addition, PET holds promise for identifying active cardiovascular lesions. Technical advances in the development of PET instruments and radiopharmaceuticals will further enhance wide applications of cardiac PET in various clinical settings.

**Acknowledgements** We thank Shiro Miura and Eriko Suzuki for their support of this study.

**Funding** This research was supported in part by a Grant-in-Aid for General Scientific Research from the Japan Society for the Promotion of Science (KAKENHI 19H03592).

## References

1. Doherty JU, Kort S, Mehran R, Schoenhagen P, Soman P, Rating Panel M, et al. ACC/AATS/AHA/ASE/ASNC/HRS/SCAI/SCCT/

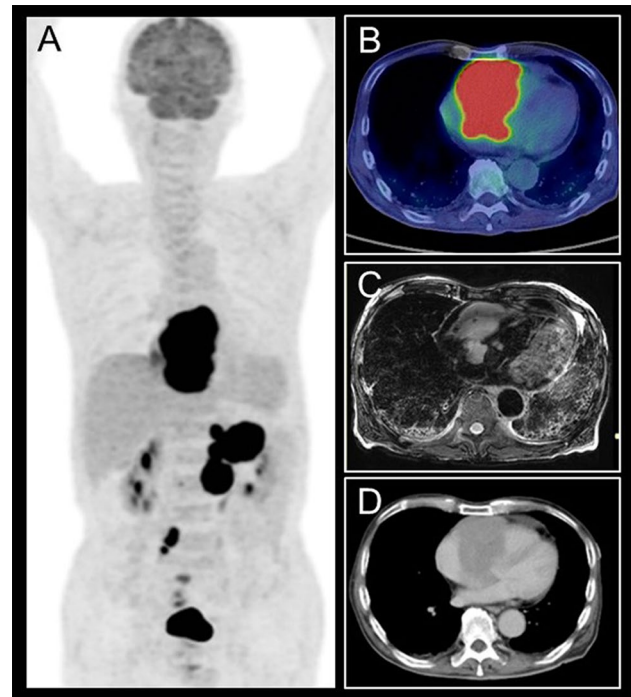


**Fig. 6** A cardiac diffuse large B-cell lymphoma. Abnormal FDG uptakes are seen in the cardiac and abdominal lesions (**a**). The cardiac lesion demonstrated very high FDG uptake (**b**; SUVmax 29.0), a relatively high intense signal in a T2-weighted image (**c**), and homogeneous enhancement on contrast-enhanced CT (**d**)

SCMR/STS 2019 Appropriate Use Criteria for Multimodality Imaging in the Assessment of Cardiac Structure and Function in Nonvalvular Heart Disease: A Report of the American College of Cardiology Appropriate Use Criteria Task Force, American Association for Thoracic Surgery, American Heart Association, American Society of Echocardiography, American Society of Nuclear Cardiology, Heart Rhythm Society, Society for Cardiovascular Angiography and Interventions, Society of Cardiovascular Computed Tomography, Society for Cardiovascular Magnetic Resonance, and the Society of Thoracic Surgeons. *J Nucl Cardiol* 2019;26(4):1392-413.

2. Bax JJ, Di Carli M, Narula J, Delgado V. Multimodality imaging in ischaemic heart failure. *Lancet*. 2019;393(10175):1056–70.
3. Manabe O, Kikuchi T, Scholte A, El Mahdiui M, Nishii R, Zhang MR, et al. Radiopharmaceutical tracers for cardiac imaging. *J Nucl Cardiol*. 2018;25(4):1204–36.
4. Gould KL, Johnson NP, Bateman TM, Beanlands RS, Bengel FM, Bober R, et al. Anatomic versus physiologic assessment of coronary artery disease. Role of coronary flow reserve, fractional flow reserve, and positron emission tomography imaging in revascularization decision-making. *J Am Coll Cardiol*. 2013;62(18):1639–53.
5. Bengel FM, Higuchi T, Javadi MS, Lautamaki R. Cardiac positron emission tomography. *J Am Coll Cardiol*. 2009;54(1):1–15.
6. Schindler TH, Dilsizian V. PET-determined hyperemic myocardial blood flow: Further progress to clinical application. *J Am Coll Cardiol*. 2014;64(14):1476–8.
7. Yoshinaga K, Tomiyama Y, Suzuki E, Tamaki N. Myocardial blood flow quantification using positron-emission tomography: analysis and practice in the clinical setting. *Circ J*. 2013;77(7):1662–711.

8. Schindler TH, Quercioli A, Valenta I, Ambrosio G, Wahl RL, Dilsizian V. Quantitative assessment of myocardial blood flow—clinical and research applications. *Semin Nucl Med.* 2014;44(4):274–93.
9. Dorbala S, Di Carli MF. Cardiac PET perfusion: prognosis, risk stratification, and clinical management. *Semin Nucl Med.* 2014;44(5):344–57.
10. Yoshinaga K, Manabe O, Tamaki N. Absolute quantification of myocardial blood flow. *J Nucl Cardiol.* 2018;25(2):635–51.
11. Mc Ardle BA, Dowsley TF, deKemp RA, Wells GA, Beanlands RS. Does rubidium-82 PET have superior accuracy to SPECT perfusion imaging for the diagnosis of obstructive coronary disease? A systematic review and meta-analysis. *J Am Coll Cardiol.* 2012;60(18):1828–37.
12. Parker MW, Iskandar A, Limone B, Perugini A, Kim H, Jones C, et al. Diagnostic accuracy of cardiac positron emission tomography versus single photon emission computed tomography for coronary artery disease: a bivariate meta-analysis. *Circ Cardiovasc Imaging.* 2012;5(6):700–7.
13. Jaarsma C, Leiner T, Bekkers SC, Crijns HJ, Wildberger JE, Nagel E, et al. Diagnostic performance of noninvasive myocardial perfusion imaging using single-photon emission computed tomography, cardiac magnetic resonance, and positron emission tomography imaging for the detection of obstructive coronary artery disease: a meta-analysis. *J Am Coll Cardiol.* 2012;59(19):1719–28.
14. Murthy VL, Naya M, Foster CR, Hainer J, Gaber M, Di Carli G, et al. Improved cardiac risk assessment with noninvasive measures of coronary flow reserve. *Circulation.* 2011;124(20):2215–24.
15. Taqueti VR, Hachamovitch R, Murthy VL, Naya M, Foster CR, Hainer J, et al. Global coronary flow reserve is associated with adverse cardiovascular events independently of luminal angiographic severity and modifies the effect of early revascularization. *Circulation.* 2015;131(1):19–27.
16. Naya M, Tamaki N, Tsutsui H. Coronary flow reserve estimated by positron emission tomography to diagnose significant coronary artery disease and predict cardiac events. *Circ J.* 2015;79(1):15–23.
17. Aikawa T, Naya M, Obara M, Manabe O, Magota K, Koyanagawa K, et al. Effects of coronary revascularization on global coronary flow reserve in stable coronary artery disease. *Cardiovasc Res.* 2019;115(1):119–29.
18. Kikuchi Y, Oyama-Manabe N, Naya M, Manabe O, Tomiyama Y, Sasaki T, et al. Quantification of myocardial blood flow using dynamic 320-row multi-detector CT as compared with (1)(5) O-H(2)O PET. *Eur Radiol.* 2014;24(7):1547–56.
19. Tomiyama Y, Manabe O, Oyama-Manabe N, Naya M, Sugimori H, Hirata K, et al. Quantification of myocardial blood flow with dynamic perfusion 3.0 Tesla MRI: validation with (15) O-water PET. *J Magn Reson Imaging.* 2015;42(3):754–62.
20. Ho KT, Ong HY, Tan G, Yong QW. Dynamic CT myocardial perfusion measurements of resting and hyperaemic blood flow in low-risk subjects with 128-slice dual-source CT. *Eur Heart J Cardiovasc Imaging.* 2015;16(3):300–6.
21. Nkoulou R, Fuchs TA, Pazhenkottal AP, Kuest SM, Ghadri JR, Stehli J, et al. Absolute myocardial blood flow and flow reserve assessed by gated SPECT with cadmium-zinc-telluride detectors using 99mTc-tetrofosmin: head-to-head comparison with 13N-ammonia PET. *J Nucl Med.* 2016;57(12):1887–922.
22. Oyama-Manabe N, Manabe O, Naya M, Kudo K, Tamaki N. Quantitative evaluation of myocardial ischemia with dynamic perfusion CT. *Ann Nucl Med.* 2019;5(1):79–83.
23. Nagara Tamaki T, Matsushima S, Yoshinaga K. Perspectives of quantitative assessments of myocardial blood flow. *Clin Transl Imaging.* 2018;6:321–7.
24. Marinescu MA, Loffler AI, Ouellette M, Smith L, Kramer CM, Bourque JM. Coronary microvascular dysfunction, microvascular angina, and treatment strategies. *JACC Cardiovasc Imaging.* 2015;8(2):210–20.
25. Zagatina A, Zhuravskaya N. The additive prognostic value of coronary flow velocity reserve during exercise echocardiography. *Eur Heart J Cardiovasc Imaging.* 2017;18(10):1179–84.
26. Ziadi MC, Dekemp RA, Williams KA, Guo A, Chow BJ, Renaud JM, et al. Impaired myocardial flow reserve on rubidium-82 positron emission tomography imaging predicts adverse outcomes in patients assessed for myocardial ischemia. *J Am Coll Cardiol.* 2011;58(7):740–8.
27. Naya M, Murthy VL, Taqueti VR, Foster CR, Klein J, Garber M, et al. Preserved coronary flow reserve effectively excludes high-risk coronary artery disease on angiography. *J Nucl Med.* 2014;55(2):248–55.
28. Camici PG, Crea F. Coronary microvascular dysfunction. *N Engl J Med.* 2007;356(8):830–40.
29. De Bruyne B, Sarma J. Fractional flow reserve: a review: invasive imaging. *Heart.* 2008;94(7):949–59.
30. Pijls NH, van Schaardenburgh P, Manoharan G, Boersma E, Bech JW, van't Veer M, et al. Percutaneous coronary intervention of functionally nonsignificant stenosis: 5-year follow-up of the DEFER Study. *J Am Coll Cardiol.* 2007; 49(21):2105–11.
31. Tonino PA, De Bruyne B, Pijls NH, Siebert U, Ikeno F, van't Veer M, et al. Fractional flow reserve versus angiography for guiding percutaneous coronary intervention. *N Engl J Med.* 2009; 360(3):213–24.
32. van Nunen LX, Zimmermann FM, Tonino PA, Barbato E, Baumbach A, Engstrom T, et al. Fractional flow reserve versus angiography for guidance of PCI in patients with multivessel coronary artery disease (FAME): 5-year follow-up of a randomised controlled trial. *Lancet.* 2015;386(10006):1853–60.
33. De Bruyne B, Baudhuin T, Melin JA, Pijls NH, Sys SU, Bol A, et al. Coronary flow reserve calculated from pressure measurements in humans. Validation with positron emission tomography. *Circulation.* 1994;89(3):1013–22.
34. Meuwissen M, Chamuleau SA, Siebes M, Schotborgh CE, Koch KT, de Winter RJ, et al. Role of variability in microvascular resistance on fractional flow reserve and coronary blood flow velocity reserve in intermediate coronary lesions. *Circulation.* 2001;103(2):184–7.
35. van de Hoef TP, van Lavieren MA, Damman P, Delewi R, Piek MA, Chamuleau SA, et al. Physiological basis and long-term clinical outcome of discordance between fractional flow reserve and coronary flow velocity reserve in coronary stenoses of intermediate severity. *Circ Cardiovasc Interv.* 2014;7(3):301–11.
36. Manabe O, Naya M, Tamaki N. Feasibility of PET for the management of coronary artery disease: comparison between CFR and FFR. *J Cardiol.* 2017;70(2):135–40.
37. Wilson RF, White CW. Does coronary artery bypass surgery restore normal maximal coronary flow reserve? The effect of diffuse atherosclerosis and focal obstructive lesions. *Circulation.* 1987;76(3):563–71.
38. Kosa I, Blasini R, Schneider-Eicke J, Dickfeld T, Neumann FJ, Ziegler S, et al. Early recovery of coronary flow reserve after stent implantation as assessed by positron emission tomography. *J Am Coll Cardiol.* 1999;34(4):1036–41.
39. Pizzuto F, Voci P, Mariano E, Puddu PE, Sardella G, Nigri A. Assessment of flow velocity reserve by transthoracic Doppler echocardiography and venous adenosine infusion before and after left anterior descending coronary artery stenting. *J Am Coll Cardiol.* 2001;38(1):155–62.
40. Nijjer SS, Petraco R, van de Hoef TP, Sen S, van Lavieren MA, Foale RA, et al. Change in coronary blood flow after percutaneous coronary intervention in relation to baseline lesion physiology: Results of the JUSTIFY-PCI study. *Circ Cardiovasc Interv.* 2015;8(6):e001715.



41. Taqueti VR, Solomon SD, Shah AM, Desai AS, Groarke JD, Osborne MT, et al. Coronary microvascular dysfunction and future risk of heart failure with preserved ejection fraction. *Eur Heart J*. 2018;39(10):840–9.
42. Aikawa T, Naya M, Koyanagawa K, Manabe O, Obara M, Magota K, et al. Improved regional myocardial blood flow and flow reserve after coronary revascularization as assessed by serial 15O-water positron emission tomography/computed tomography. *Eur Heart J Cardiovasc Imaging*. 2020;21(1):36–46.
43. Tillisch J, Brunken R, Marshall R, Schwaiger M, Mandelkern M, Phelps M, et al. Reversibility of cardiac wall-motion abnormalities predicted by positron tomography. *N Engl J Med*. 1986;314(14):884–8.
44. Tamaki N, Yonekura Y, Yamashita K, Saji H, Magata Y, Senda M, et al. Positron emission tomography using fluorine-18 deoxyglucose in evaluation of coronary artery bypass grafting. *American J Cardiol*. 1989;64(14):860–5.
45. Tamaki N, Kawamoto M, Tadamura E, Magata Y, Yonekura Y, Nohara R, et al. Prediction of reversible ischemia after revascularization. Perfusion and metabolic studies with positron emission tomography. *Circulation*. 1995;91(6):1697–705.
46. Allman KC, Shaw LJ, Hachamovitch R, Udelson JE. Myocardial viability testing and impact of revascularization on prognosis in patients with coronary artery disease and left ventricular dysfunction: a meta-analysis. *J Am Coll Cardiol*. 2002;39(7):1151–8.
47. Juneau D, Erthal F, Alzahrani A, Alenazy A, Nery PB, Beanlands RS, et al. Systemic and inflammatory disorders involving the heart: the role of PET imaging. *Q J Nucl Med Mol Imaging*. 2016;60(4):383–96.
48. Kang SS, Gosselin C, Ren D, Greisler HP. Selective stimulation of endothelial cell proliferation with inhibition of smooth muscle cell proliferation by fibroblast growth factor-1 plus heparin delivered from fibrin glue suspensions. *Surgery*. 1995;118(2):280–6 (**discussion 6-7**).
49. Scholtens AM, Verberne HJ, Budde RP, Lam MG. Additional heparin preadministration improves cardiac glucose metabolism suppression over low-carbohydrate diet alone in (1)(8)F-FDG PET imaging. *J Nucl Med*. 2016;57(4):568–73.
50. Manabe O, Yoshinaga K, Ohira H, Masuda A, Sato T, Tsujino I, et al. The effects of 18-h fasting with low-carbohydrate diet preparation on suppressed physiological myocardial (18)F-fluorodeoxyglucose (FDG) uptake and possible minimal effects of unfractionated heparin use in patients with suspected cardiac involvement sarcoidosis. *J Nucl Cardiol*. 2016;23(2):244–52.
51. Tam MC, Patel VN, Weinberg RL, Hulten EA, Aaronson KD, Pagani FD, et al. Diagnostic accuracy of FDG PET/CT in suspected LVAD infections: a case series, systematic review, and meta-analysis. *JACC Cardiovasc Imaging*. 2020;13(5):1191–202.
52. Doughan AR, Williams BR. Cardiac sarcoidosis. *Heart*. 2006;92(2):282–8.
53. Mehta D, Lubitz SA, Frankel Z, Wisnivesky JP, Einstein AJ, Goldman M, et al. Cardiac involvement in patients with sarcoidosis: diagnostic and prognostic value of outpatient testing. *Chest*. 2008;133(6):1426–35.
54. Kumita S, Yoshinaga K, Miyagawa M, Momose M, Kiso K, Kasai T, et al. Recommendations for (18)F-fluorodeoxyglucose positron emission tomography imaging for diagnosis of cardiac sarcoidosis-2018 update: Japanese Society of Nuclear Cardiology recommendations. *J Nucl Cardiol*. 2019;26(4):1414–33.
55. Ishimaru S, Tsujino I, Takei T, Tsukamoto E, Sakaue S, Kamigaki M, et al. Focal uptake on 18F-fluoro-2-deoxyglucose positron emission tomography images indicates cardiac involvement of sarcoidosis. *Eur Heart J*. 2005;26(15):1538–43.
56. Ohira H, Tsujino I, Yoshinaga K. (1)(8)F-Fluoro-2-deoxyglucose positron emission tomography in cardiac sarcoidosis. *Eur J Nucl Med Mol Imaging*. 2011;38(9):1773–83.
57. Yamagishi H, Shirai N, Takagi M, Yoshiyama M, Akioka K, Takeuchi K, et al. Identification of cardiac sarcoidosis with (13)N-NH(3)/(18)F-FDG PET. *J Nucl Med*. 2003;44(7):1030–6.
58. Okumura W, Iwasaki T, Toyama T, Iso T, Arai M, Oriuchi N, et al. Usefulness of fasting 18F-FDG PET in identification of cardiac sarcoidosis. *J Nucl Med*. 2004;45(12):1989–98.
59. Birnie DH, Sauer WH, Bogun F, Cooper JM, Culver DA, Duvernoy CS, et al. HRS expert consensus statement on the diagnosis and management of arrhythmias associated with cardiac sarcoidosis. *Heart Rhythm*. 2014;11(7):1305–23.
60. Ishida Y, Yoshinaga K, Miyagawa M, Moroi M, Kondoh C, Kiso K, et al. Recommendations for (18)F-fluorodeoxyglucose positron emission tomography imaging for cardiac sarcoidosis: Japanese Society of Nuclear Cardiology recommendations. *Ann Nucl Med*. 2014;28(4):393–403.
61. Ordovas KG, Higgins CB. Delayed contrast enhancement on MR images of myocardium: past, present, future. *Radiology*. 2011;261(2):358–74.
62. Manabe O, Oyama-Manabe N, Ohira H, Tsutsui H, Tamaki N. Multimodality evaluation of cardiac sarcoidosis. *J Nucl Cardiol*. 2012;19(3):621–4.
63. Ohira H, Birnie DH, Pena E, Bernick J, Mc Ardle B, Leung E, et al. Comparison of (18)F-fluorodeoxyglucose positron emission tomography (FDG PET) and cardiac magnetic resonance (CMR) in corticosteroid-naïve patients with conduction system disease due to cardiac sarcoidosis. *Eur J Nucl Med Mol Imaging*. 2016;43(2):259–69.
64. Kouranos V, Tzelepis GE, Rapti A, Mavrogeni S, Aggeli K, Douskou M, et al. Complementary role of CMR to conventional screening in the diagnosis and prognosis of cardiac sarcoidosis. *JACC Cardiovasc Imaging*. 2017;10(12):1437–47.
65. Blankstein R, Osborne M, Naya M, Waller A, Kim CK, Murthy VL, et al. Cardiac positron emission tomography enhances prognostic assessments of patients with suspected cardiac sarcoidosis. *J Am Coll Cardiol*. 2014;63(4):329–36.
66. Manabe O, Yoshinaga K, Ohira H, Sato T, Tsujino I, Yamada A, et al. Right ventricular (18)F-FDG uptake is an important indicator for cardiac involvement in patients with suspected cardiac sarcoidosis. *Ann Nucl Med*. 2014;28(7):656–67.
67. Norikane T, Yamamoto Y, Maeda Y, Noma T, Dobashi H, Nishiyama Y. Comparative evaluation of (18)F-FLT and (18)F-FDG for detecting cardiac and extra-cardiac thoracic involvement in patients with newly diagnosed sarcoidosis. *EJNMMI Res*. 2017;7(1):69.
68. Martineau P, Pelletier-Galarneau M, Juneau D, Leung E, Nery PB, de Kemp R, et al. Imaging cardiac sarcoidosis with FLT-PET compared with FDG/Perfusion-PET: a prospective pilot study. *JACC Cardiovasc Imaging*. 2019;12(11 Pt 1):2280–1.
69. Manabe O, Hirata K, Shozo O, Shiga T, Uchiyama Y, Kobayashi K, et al. (18)F-fluoromisonidazole (FMISO) PET may have the potential to detect cardiac sarcoidosis. *J Nucl Cardiol*. 2017;24(1):329–31.
70. Furuya S, Naya M, Manabe O, Hirata K, Ohira H, Aikawa T, et al. (18)F-FMISO PET/CT detects hypoxic lesions of cardiac and extra-cardiac involvement in patients with sarcoidosis. *J Nucl Cardiol*. 2019. <https://doi.org/10.1007/s12350-019-01976-6>.
71. Van Riet J, Hill EE, Gheysens O, Dymarkowski S, Herregods MC, Herijgers P, et al. (18)F-FDG PET/CT for early detection of embolism and metastatic infection in patients with infective endocarditis. *Eur J Nucl Med Mol Imaging*. 2010;37(6):1189–97.
72. Saby L, Laas O, Habib G, Cammilleri S, Mancini J, Tessonnier L, et al. Positron emission tomography/computed tomography for diagnosis of prosthetic valve endocarditis: increased valvular 18F-fluorodeoxyglucose uptake as a novel major criterion. *J Am Coll Cardiol*. 2013;61(23):2374–82.

73. Asmar A, Ozcan C, Diederichsen AC, Thomassen A, Gill S. Clinical impact of 18F-FDG-PET/CT in the extra cardiac work-up of patients with infective endocarditis. *Eur Heart J Cardiovasc Imaging*. 2014;15(9):1013–9.
74. Pizzi MN, Roque A, Fernandez-Hidalgo N, Cuellar-Calabria H, Ferreira-Gonzalez I, Gonzalez-Alujas MT, et al. Improving the diagnosis of infective endocarditis in prosthetic valves and intracardiac devices with 18F-fluorodeoxyglucose positron emission tomography/computed tomography angiography: initial results at an infective endocarditis referral center. *Circulation*. 2015;132(12):1113–26.
75. Jimenez-Ballve A, Perez-Castejon MJ, Delgado-Bolton RC, Sanchez-Enrique C, Vilacosta I, Vivas D, et al. Assessment of the diagnostic accuracy of (18)F-FDG PET/CT in prosthetic infective endocarditis and cardiac implantable electronic device infection: comparison of different interpretation criteria. *Eur J Nucl Med Mol Imaging*. 2016;43(13):2401–12.
76. Mahmood M, Kendi AT, Ajmal S, Farid S, O'Horo JC, Chareonthaitawee P, et al. Meta-analysis of 18F-FDG PET/CT in the diagnosis of infective endocarditis. *J Nucl Cardiol*. 2019;26(3):922–35.
77. Bruls S, Courtois A, Nusgens B, Defraigne JO, Delvenne P, Hustinx R, et al. 18F-FDG PET/CT in the management of aortitis. *Clin Nucl Med*. 2016;41(1):28–33.
78. van der Valk FM, Verweij SL, Zwinderman KA, Strang AC, Kaiser Y, Marquering HA, et al. Thresholds for arterial wall inflammation quantified by (18)F-FDG PET Imaging: implications for vascular interventional studies. *JACC Cardiovasc Imaging*. 2016;9(10):1198–207.
79. Yabusaki S, Oyama-Manabe N, Manabe O, Hirata K, Kato F, Miyamoto N, et al. Characteristics of immunoglobulin G4-related aortitis/periaortitis and periarteritis on fluorodeoxyglucose positron emission tomography/computed tomography co-registered with contrast-enhanced computed tomography. *EJNMMI Res*. 2017;7(1):20.
80. Oyama-Manabe N, Yabusaki S, Manabe O, Kato F, Kanno-Okada H, Kudo K. IgG4-related cardiovascular disease from the aorta to the coronary arteries: multidetector CT and PET/CT. *Radiographics*. 2018;38(7):1934–48.
81. Mikail N, Benali K, Dossier A, Bouleti C, Hyafil F, Le Guludec D, et al. Additional diagnostic value of combined angio-computed tomography and (18)F-fluorodeoxyglucose positron emission tomography in infectious aortitis. *JACC Cardiovasc Imaging*. 2018;11(2 Pt 2):361–4.
82. Olthof SC, Krumm P, Henes J, Nikolaou K, la Fougere C, Pfannenbergen C, et al. Imaging giant cell arteritis and aortitis in contrast enhanced 18F-FDG PET/CT: which imaging score correlates best with laboratory inflammation markers? *Eur J Radiol*. 2018;99:94–102.
83. Padoan R, Crimi F, Felicetti M, Padovano F, Lacognata C, Stramare R, et al. Fully integrated 18F-FDG PET/MR in large vessel vasculitis. *Q J Nucl Med Mol Imaging*. 2019. <https://doi.org/10.23736/S1824-4785.19.03184-4>.
84. Rahbar K, Seifarth H, Schafers M, Stegger L, Hoffmeier A, Spieker T, et al. Differentiation of malignant and benign cardiac tumors using 18F-FDG PET/CT. *J Nucl Med*. 2012;53(6):856–63.
85. Kikuchi Y, Oyama-Manabe N, Manabe O, Naya M, Ito YM, Hatanaka KC, et al. Imaging characteristics of cardiac dominant diffuse large B-cell lymphoma demonstrated with MDCT and PET/CT. *Eur J Nucl Med Mol Imaging*. 2013;40(9):1337–444.
86. Nensa F, Tezgah E, Poeppel TD, Jensen CJ, Schelhorn J, Kohler J, et al. Integrated 18F-FDG PET/MR imaging in the assessment of cardiac masses: a pilot study. *J Nucl Med*. 2015;56(2):255–60.
87. Krumm P, Mangold S, Gatidis S, Nikolaou K, Nensa F, Bamberg F, et al. Clinical use of cardiac PET/MRI: current state-of-the-art and potential future applications. *Jpn J Radiol*. 2018;36(5):313–23.
88. Manabe O, Oyama-Manabe N, Nagai T, Furuya S, Anzai T. Detailed visualization of the right and left ventricular, left atrial, and epicardial involvement of cardiac sarcoidosis with novel semiconductor PET/CT. *Eur J Nucl Med Mol Imaging*. 2020;47(7):1773–4.

**Publisher's Note** Springer Nature remains neutral with regard to jurisdictional claims in published maps and institutional affiliations.